Localization of Cell Wall Polysaccharides in Normal and Compression Wood of Radiata Pine: Relationships with Lignification and Microfibril Orientation[1]

Lloyd A. Donaldson* and J. Paul Knox

Scion, Rotorua 3010, New Zealand (L.A.D.); and Centre for Plant Sciences, Faculty of Biological Sciences, University of Leeds, Leeds LS2 9JT, United Kingdom (J.P.K.)

The distribution of noncellulosic polysaccharides in cell walls of tracheids and xylem parenchyma cells in normal and compression wood of *Pinus radiata*, was examined to determine the relationships with lignification and cellulose microfibril orientation. Using fluorescence microscopy combined with immunocytochemistry, monoclonal antibodies were used to detect xyloglucan (LM15), β(1,4)-galactan (LM5), heteroxylan (LM10 and LM11), and galactoglucomannan (LM21 and LM22). Lignin and crystalline cellulose were localized on the same sections used for immunocytochemistry by autofluorescence and polarized light microscopy, respectively. Changes in the distribution of noncellulosic polysaccharides between normal and compression wood were associated with changes in lignin distribution. Increased lignification of compression wood secondary walls was associated with novel deposition of β(1,4)-galactan and with reduced amounts of xylan and mannan in the outer S2 (S2L) region of tracheids. Xylan and mannan were detected in all lignified xylem cell types (tracheids, ray tracheids, and thick-walled ray parenchyma) but were not detected in unlignified cell types (thin-walled ray parenchyma and resin canal parenchyma). Mannan was absent from the highly lignified compound middle lamella, but xylan occurred throughout the cell walls of tracheids. Using colocalization measurements, we confirmed that polysaccharides containing galactose, mannose, and xylose have consistent correlations with lignification. Low or unsubstituted xylans were localized in cell wall layers characterized by transverse cellulose microfibril orientation in both normal and compression wood tracheids. Our results support the theory that the assembly of wood cell walls, including lignification and microfibril orientation, may be mediated by changes in the amount and distribution of noncellulosic polysaccharides.

The cell walls of secondary xylem are complex composites of cellulose, hemicelluloses, pectins, and lignin. Composition varies among cell wall layers, cell types, and in response to gravitropic stimulus (Timell, 1986; Donaldson, 2001). In addition to variations in composition among wall layers, there are also variations in ultrastructure, most notably cellulose microfibril orientation (Donaldson, 2008).

During the formation of tracheids, the major cell type in conifer wood, polysaccharides, including cellulose, are deposited as secondary cell walls with three regions known as the S1, S2, and S3 layers (Wardrop and Preston, 1947). This is followed by addition of lignin in a distinctive pattern, beginning in the outer middle lamella/primary wall and gradually progressing across the secondary wall to the lumen (Donaldson, 2001). The compound middle lamella is normally more highly lignified than the secondary wall, but this pattern is significantly modified in compression wood, with a reduction in lignification of the middle lamella and increased lignification of the outer secondary wall (Donaldson, 2001). The mechanisms underlying the control of lignin deposition are not well understood, but it is clear that the pattern of lignification cannot be accounted for by simple diffusion of monomers into the developing wall (Davin and Lewis, 2005; Ralph et al., 2008).

The orientation of cellulose microfibrils also varies between wall layers. In the S1 and S3 layers, microfibrils are almost horizontal with respect to the fiber axis, while in the thicker S2 layer, microfibril orientation has a more vertical orientation that varies with cambial age and gravitropic stimulus (Donaldson, 2008). Microfibrils are produced by synthetic complexes called rosettes that are localized to the plasma membrane (Kimura et al., 1999). The organization of these rosettes is thought to be controlled in part by their abundance, which may determine packing arrangements and thereby influence microfibril orientation (Emons et al., 2002). Orientation of microtubules in the cytoskeleton has been shown to match that of adjacent microfibrils, but it is not clear what determines the orientation of the cytoskeleton or why it changes during secondary cell wall development (Baskin, 2001; Spokevicius et al., 2007; Wightman and

[1] This work was supported by the New Zealand Ministry of Science and Innovation (grant nos. C04X0207 and C04X0703).

* Corresponding author; e-mail lloyd.donaldson@scionresearch.com.

The author responsible for distribution of materials integral to the findings presented in this article in accordance with the policy described in the Instructions for Authors (www.plantphysiol.org) is: Lloyd A. Donaldson (lloyd.donaldson@scionresearch.com).

www.plantphysiol.org/cgi/doi/10.1104/pp.111.184036

 © 2011 American Society of Plant Biologists. All Rights Reserved.

Turner, 2008). The mechanism by which changes in cellulose orientation between wall layers are controlled is not known.

The noncellulosic polysaccharides of conifer (Coniferae) xylem are primarily composed of Ara, Gal, Glc, Man, and Xyl. Arabinogalactan proteins, galacturonans, and xyloglucans are characteristic of primary cell walls in conifer xylem (Putoczki et al., 2007, 2008; Hsieh et al., 2009) while arabino-4-*O*-methylglucuronoxylan and *O*-acetyl-galactoglucomannan are the main noncellulosic polysaccharides of secondary cell walls (Melton et al., 2009). In compression wood, the amounts of xylan and mannan are reduced relative to normal wood. By contrast, β(1,4)-galactan is found almost exclusively in compression wood (Timell, 1986; Mast et al., 2009; Nanayakkara et al., 2009).

There is considerable evidence for interactions among cell wall components. Mannans, especially polymers with fewer Gal side chains and reduced acetylation, associate strongly with cellulose (Mishima et al., 1998; Hannuksela et al., 2002). In a comparison of different polysaccharides, Iwata et al. (1998) found that beech (*Fagus sylvatica*) glucomannans have the highest affinity for cellulose, followed by xyloglucan, xylan, and arabinogalactan. Mannans may also associate with xylans and with lignin (Lawoko et al., 2005; Barakat et al., 2007).

The development of glycan-directed probes, such as monoclonal antibodies and carbohydrate-binding modules, has made it possible to characterize the location of different components in cell walls (Willats et al., 2000; Boraston et al., 2004; Knox, 2008; Donaldson, 2009).

Both monoclonal and polyclonal antibodies have been used to localize mannans in the secondary walls of tracheids in a number of conifer species. Glucomannan is localized to the secondary wall of tracheids with increased deposition at the S1/S2 boundary and is deposited prior to lignification in both normal and compression wood (Maeda et al., 2000; Hosoo et al., 2006; Altaner et al., 2007b; Fernando and Daniel, 2008; Kim et al., 2010b, 2011).

Glucuronoxylans are the main constituents of hardwood hemicellulose but are less abundant components of softwood cell walls (Timell, 1967; Nanayakkara et al., 2009; Kim et al., 2010c). Altaner et al. (2010) have examined the distribution of heteroxylans in radiata pine (*Pinus radiata*) by immunoelectron microscopy showing unsubstituted xylans (LM10) in the S1 and S3 layers and more highly substituted xylans (LM11) across all areas of the cell wall except the primary wall. Filonova et al. (2007) also demonstrated a generalized distribution of labeled xylan-binding modules across cell walls on Scots pine (*Pinus sylvestris*) wood sections.

β(1,4)-Galactan has been immunolocalized in a number of studies on compression wood using the LM5 monoclonal antibody (Schmitt et al., 2006; Altaner et al., 2007a, 2010; Mast et al., 2009; Kim et al., 2010a). These studies have shown that galactan is associated with the highly lignified region of the outer secondary wall in this wood type, while in normal wood, the LM5 epitope is absent (Mast et al., 2009; Kim et al., 2010a).

Several hypotheses have emerged as a result of these studies on secondary xylem that suggest an involvement of noncellulosic polysaccharides as regulators/facilitators of cell wall assembly. Xylans may function as twisting agents, acting at the boundary between cell wall layers where microfibril angle is changing (Reis and Vian, 2004). Xylans have been specifically localized to the transition zone between the S1 and S2 layers and may act as helper molecules controlling the orientation, aggregation, and alignment of microfibrils (Reis and Vian, 2004).

Similarly, variations in lignification across cell walls have been related to changes in hemicellulose and pectins, especially in relation to the deposition of β(1,4)-galactan in the reaction wood of conifers (Schmitt et al., 2006; Altaner et al., 2007a, 2010; Mast et al., 2009; Kim et al., 2010a). Studies of artificial lignins synthesized in vitro have shown that polysaccharides can influence the way in which lignin polymerizes (Tanahashi and Higuchi, 1990; Yoshida et al., 1994; Lairez et al., 2005).

Normal and compression wood show substantial differences in composition and ultrastructure and offer a unique opportunity to study the potential role(s) of noncellulosic polysaccharides in lignification and the orientation of cellulose microfibrils by examining the relationships among cell wall components in these two wood types. We used immunocytochemistry combined with lignin autofluorescence and polarized light microscopy to examine the relationships among cell wall components in these two wood types. The correlations among cell wall components that we observed suggest that noncellulosic polysaccharides are associated with changes in lignin concentration and microfibril angle that occur across the tracheid cell wall and hence may play a role in controlling lignification and microfibril orientation in secondary cell walls.

RESULTS

Immunolocalization of Cell Wall Polysaccharides in Normal and Compression Wood

We sought to examine the distribution of noncellulosic polysaccharides in normal and compression wood (Fig. 1) using six monoclonal antibodies raised against xyloglucan, galactan, heteroxylans, and mannan as described in the following paragraphs. For all experiments described below, negative control samples, where the primary antibody was omitted, indicated that there was no nonspecific binding of the secondary antibody (data shown only for the LM21 mannan primary antibody and Alexa568-labeled secondary antibody in Fig. 2). These controls also demonstrated the lack of any significant contribution of lignin autofluorescence to the captured immunolabeled images. The fluorescence from the Alexa568 and

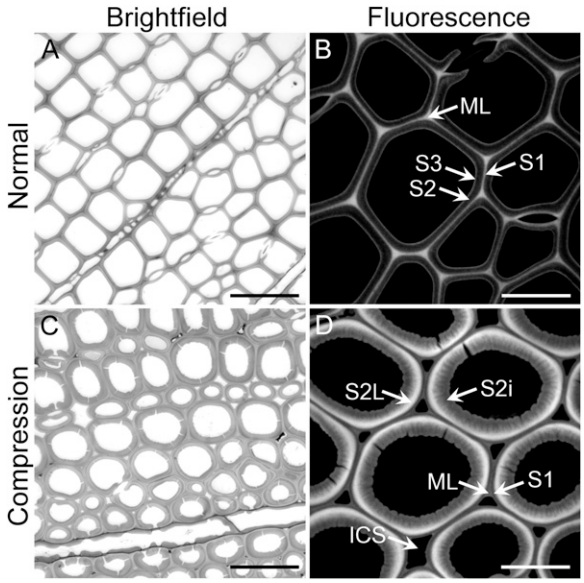

Figure 1. Comparison of bright-field and fluorescence images of normal and compression wood. Bright-field samples are stained with toluidine blue. Fluorescence images show lignin autofluorescence in all cell wall layers. A, Normal wood in transverse view showing earlywood cell walls. Bar = 60 μm. B, Normal wood in transverse view showing lignin autofluorescence (ML, middle lamella + primary wall, S1, S2, and S3 layers of the secondary cell wall). Bar = 20 μm. C, Compression wood in transverse view showing early wood cell walls. Bar = 60 μm. D, Compression wood in transverse view showing lignin autofluorescence at the same exposure as B (S2L, highly lignified outer S2 layer; S2i, less lignified inner S2 layer; ICS, intercellular space). Bar = 20 μm.

Alexa647 dyes used to label the secondary antibody is therefore significantly brighter than lignin autofluorescence in both wood types.

The LM15 antibody is directed to the XXXG motif of xyloglucan (Marcus et al., 2008). In both normal wood and compression wood, the LM15 epitope was specifically detected only in the primary walls of tracheids (Fig. 3, A and B).

The LM10 antibody is directed to low or unsubstituted xylans with no reactivity to arabinoxylan (McCartney et al., 2005). In normal wood, the LM10 epitope was detected mainly in the S1 and S3 layers of the secondary wall, at pit borders, and often in the middle lamella at the cell corners (Fig. 3C). In compression wood, the LM10 epitope was detected at the primary wall/S1 boundary, the inner S2 layer (S2i), and in the middle lamella at the cell corners (Fig. 3D).

The LM11 antibody binds to both unsubstituted xylan and arabinoxylan (McCartney et al., 2005). In normal wood, the LM11 epitope was detected throughout the primary and secondary cell walls, showing increased abundance in the S1 and S3 layers of secondary cell walls (Fig. 3E), which probably corresponds to the less substituted xylans detected by LM10 (Fig. 3C). In compression wood, the LM11 epitope was detected throughout the primary and secondary cell walls but was sparse or absent in the outer S2 region of secondary cell walls (Fig. 3F).

Taken together, the results from these two antibodies suggest that xylan substitution appears to vary across the secondary wall. Less substituted xylans appear to be more predominant in the S1 and S3 regions, in normal wood, and in the S1 and inner S2 regions of compression wood, as demonstrated by increased binding of LM10 relative to LM11.

The LM5 antibody is directed against β(1,4)-galactan (Jones et al., 1997). In normal wood, the LM5 epitope was sparsely distributed in the primary walls of tracheids (Fig. 3G). In compression wood, the LM5 epitope was abundant in the outer part of the S2 layer and was also observed with reduced abundance in the S1 layer (Fig. 3H) of the secondary cell wall of tracheids.

In this study, mannan was detected with the LM21 and LM22 monoclonal antibodies, which are known to bind to mannan, glucomannan, legume seed galactomannan, and mannan/glucomannan (Marcus et al., 2010). Both LM21 and LM22 bound in an equivalent manner to three samples of galactoglucomannan obtained from pine wood (data not shown). However, there were some differences in the distribution of the two epitopes in the immunolabeling of wood sections.

In normal wood, the LM21 epitope was detected in the S1 and S2 layers of the secondary wall of tracheids. The LM21 epitope was often more abundant at the S1/S2 boundary, but there was weak or no binding in the

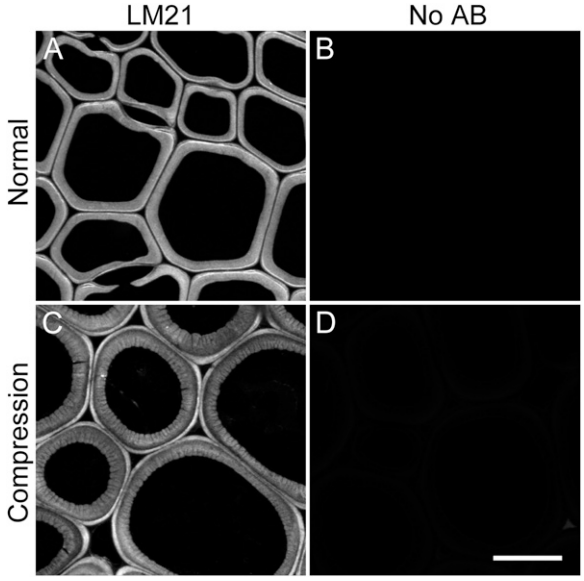

Figure 2. Immunolocalization images of normal and compression wood experiments with and without primary LM21 (mannan) antibody. A, Normal wood in transverse view showing LM21 epitope localization. B, Normal wood negative control image lacking primary antibody (AB), at the same exposure as A. C, Compression wood in transverse view showing LM21 epitope localization. D, Compression wood negative control image lacking primary antibody, at the same exposure as C. Bar = 20 μm.

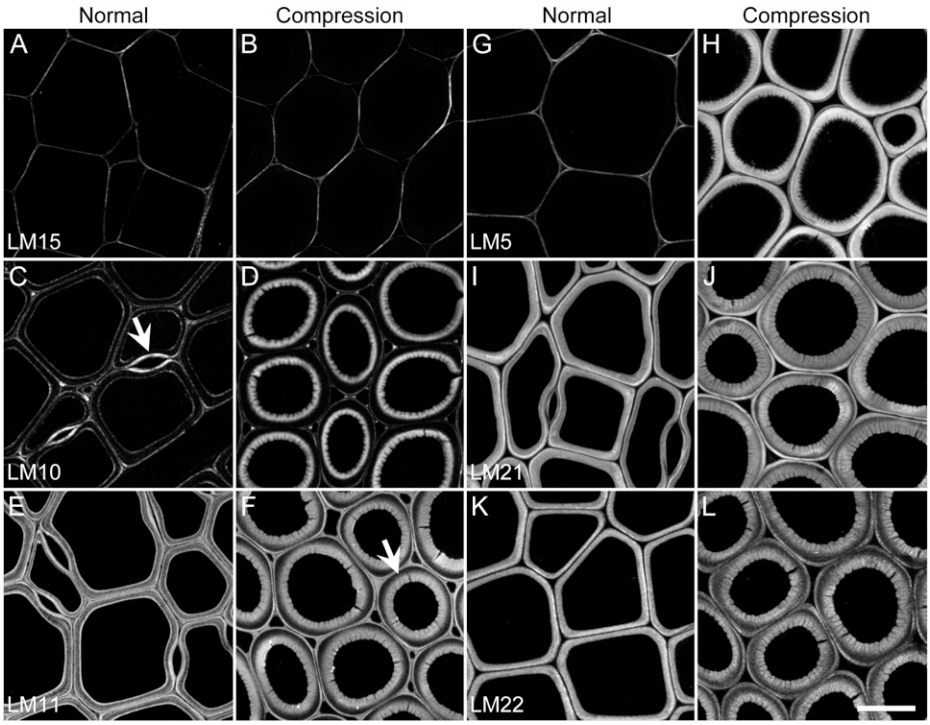

Figure 3. Immunolocalization of polysaccharides in transverse sections of normal wood (A, C, E, G, I, and K) and compression wood (B, D, F, H, J, and L). A and B, LM15 (xyloglucan) epitope showing localization in the primary cell walls of tracheids in both wood types. C, LM10 (low and unsubstituted xylan) epitope showing localization in the S1 and S3 layers in normal wood tracheids and high abundance at pit borders (arrow). D, LM10 epitope in compression wood tracheids, showing localization in the middle lamella at the cell corners, in the S1 layer, and in the inner region of the S2 layer. E, LM11 (unsubstituted and highly substituted xylan and arabinoxylan) epitope in normal wood, showing localization throughout the primary and secondary cell walls of tracheids, with stronger label in the S1 and S3 layers of the secondary cell wall. F, LM11 epitope in compression wood showing distribution throughout the cell wall, with the exception of the outer S2 region (arrow). G and H, LM5 [β(1,4)-Galactan] epitope, showing sparse localization in the primary wall of normal wood tracheids (G) but abundant distribution in the outer secondary wall of compression wood tracheids (H). I, LM21 (galactoglucomannan) epitope in normal wood, showing localization in the secondary cell wall of tracheids with increased abundance in some areas of the S1 layer. J, LM21 epitope in compression wood tracheids, showing localization across the secondary wall, with increased abundance in the S1 region and reduced abundance in the outer S2L region. K and L, LM22 (galactoglucomannan) epitope, showing distribution in a similar pattern to the LM21 epitope. Bar = 20 μm.

S3 region (Fig. 3I). In compression wood, the LM21 epitope was abundant in secondary cell walls of tracheids, with greater abundance in the S1 region and reduced abundance in the outer S2 region (Fig. 3J). LM22 showed essentially the same distribution as LM21, but with slight differences that confirm that the LM22 epitope is not identical to LM21 (Fig. 3, K and L). The LM22 epitope is less abundant in the outer S2 region of compression wood, but the increased abundance at the S1/S2 boundary in normal wood is less obvious compared to LM21 (Fig. 3, I and J). The exact nature of these differences in binding patterns in terms of mannan structures remains unresolved.

Detection of Polysaccharides in Rays and Resin Canals

In radiata pine, rays contain three types of cells. Ray parenchyma cells have thin unlignified primary walls, while less common thick-walled ray parenchyma cells have secondary walls and are lignified. Rays also contain ray tracheids that have secondary walls and are lignified. In both normal wood and compression wood, all ray cells contain xyloglucan (Fig. 4A) and galactan in their primary cell walls. The LM15 epitope (xyloglucan) appears to be more abundant in the primary cell walls of unlignified ray cells (Fig. 4A) compared to lignified ray cells and axial tracheids. Lignified ray cells also contain mannan (Fig. 4B) and xylan in their secondary cell walls. Both LM10 and LM11 epitopes are particularly abundant in the secondary walls of ray tracheids (Fig. 4C).

In resin canal parenchyma cells, which have unlignified primary walls, LM5 (galactan) and LM15 (xyloglucan) epitopes are abundant relative to the primary walls of axial tracheids (Fig. 4, D and E). The LM5 epitope seems to be sparse in the primary walls of epithelial cells relative to other resin canal tissues (Fig. 4D). The LM15 epitope appears to be

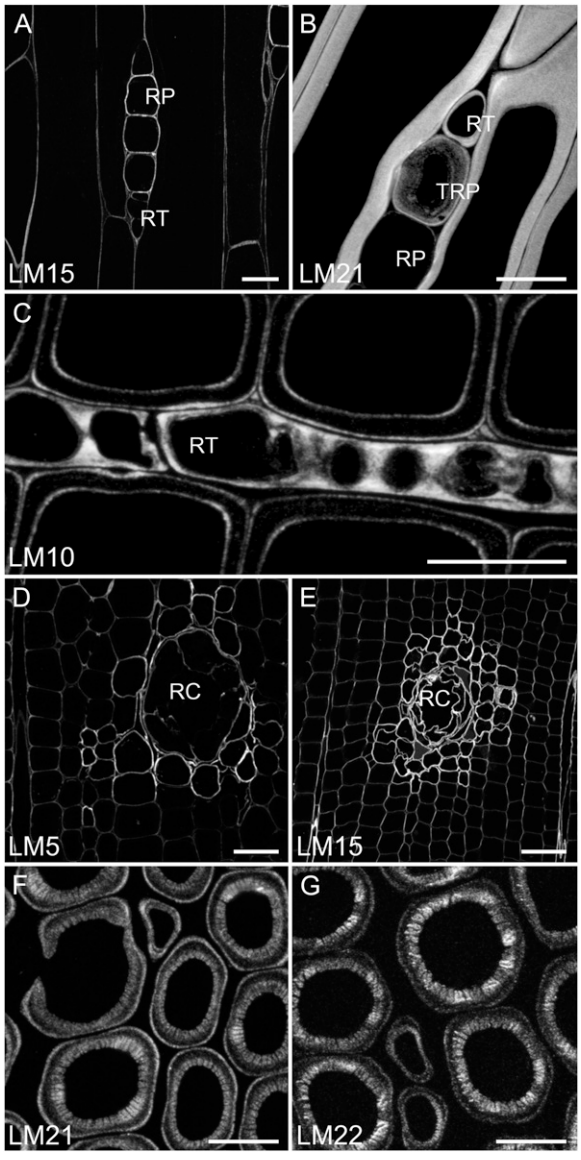

Figure 4. Immunolocalization of polysaccharides in rays, resin canals, and delignified tracheids. A, LM15 (xyloglucan) epitope is abundant in primary walls of unlignified ray parenchyma cells (RP) and slightly less abundant in primary walls of ray tracheids (RT) and axial tracheids (tangential longitudinal view). Bar = 20 μm. B, LM21 (galactoglucomannan) epitope is detected in secondary walls of ray tracheids (RT) and thick-walled ray parenchyma cells (TRP) both of which are lignified (tangential longitudinal view). Bar = 20 μm. C, LM10 (low or unsubstituted xylan) epitope is abundant in the secondary wall of ray tracheids (transverse view). Bar = 20 μm. D, LM5 [β(1,4)-galactan] epitope is abundant in the primary walls of resin canal (RC) parenchyma cells but sparse in the epithelial cells (transverse view). Bar = 40 μm. E, LM15 (xyloglucan) epitope is abundant in the primary walls of both resin canal (RC) parenchyma and epithelial cells but is less abundant in the primary wall of axial tracheids (transverse view). Bar = 80 μm. F, LM21 and G, LM22 (galactoglucomannan) epitope shows the same pattern of distribution in delignified compression wood tracheids as in untreated tracheids (transverse view). Bar = 20 μm.

equally abundant in epithelial cells compared to resin canal parenchyma cells (Fig. 4E). To investigate the potential role of epitope masking in the differential detection of LM5 and LM15 epitopes between tracheids, rays, and resin canals, we briefly examined the capacity of pectic homogalacturonan (Marcus et al., 2008) and lignin to mask LM15 detection in a sample containing cambium and differentiating and mature xylem. Sections were examined before and after treatment with 0.1 M sodium carbonate at high pH combined with pectinase enzyme treatment (Hervé et al., 2011). LM19, an antibody against pectic homogalacturonan, was used to check the effectiveness of enzyme treatment (Hervé et al., 2011). Enzyme treatment was found to effectively remove homogalacturonan from both lignified and unlignified tissues, but this had no obvious effect on LM15 epitope detection, suggesting that masking of xyloglucan by homogalacturonan (Marcus et al., 2008) is unlikely to account for the greater frequency of LM15 epitope in ray and resin canal tissue.

Likewise, there was no indication of reduced amounts of LM15 epitope between differentiating tracheids and fully lignified tissue; in fact, the epitope seemed to be more frequent in lignified primary walls of tracheids compared to those undergoing secondary wall formation. We conclude that primary walls in ray parenchyma and resin canal parenchyma tissues contain more xyloglucan than the primary walls of lignified tracheids. For the LM5 epitope, there was a slight decrease in detection with the onset of lignification (Mast et al., 2009), suggesting that lignin masking may account in part for the observed increase in LM5 epitope in ray and resin canal tissue, but this does not discount the possibility that these cell walls simply contain more of this epitope.

Detection of Polysaccharides in Delignified Cell Walls

Delignification of compression wood resulted in the loss of the LM15 xyloglucan, LM5 galactan, and the LM10/LM11 xylan epitopes but not those of the two mannan epitopes LM21 and LM22 (Fig. 4, F and G). Delignification treatment is known to also remove hemicelluloses, including mannans, in addition to lignin and can also modify polysaccharide structures. Thus, the loss of some epitopes can be attributed to epitope destruction or modification rather than loss due to linkage with lignin. The retention of some mannan epitopes in the delignified cell walls is probably the result of mannan binding to cellulose during the lignin removal process. Mannan is known to have a strong affinity for cellulose compared to other polysaccharides (Iwata et al., 1998). These two mannan epitopes showed similar distributions in delignified cell walls to those observed in untreated compression wood, demonstrating that reduced labeling of epitope in the outer S2 region of compression wood is not due to reduced access resulting from increased lignification and reflects a real reduction in epitope in this region. Similar results were found for delignified normal wood.

Colocalization of Lignin and Polysaccharides

Colocalization analysis can be carried out using a variety of methods. In this study, we used the commonly used procedures described by Bolte and Cordelières (2006). It is important to note we colocalized only in two dimensions as the antibodies are restricted entirely to the surface of the sections. Pearson correlation provides a measure of the correlation between the red (polysaccharide epitopes) and green (lignin) components of fluorescence images reflecting the correlation between red and green intensities within the cell wall and, thus, excluding the lumen pixels. This value is informative when relating polysaccharide epitope location to degree of lignification (Table I), a positive correlation indicating high epitope intensity associated with high lignin intensity, and a negative correlation indicating high epitope intensity associated with low lignin intensity. Manders overlap coefficient is based on the Pearson correlation with values varying from 0 to 1, the former corresponding to nonoverlapping images and the latter indicating 100% colocalization between both images. M1 represents the fraction of polysaccharide overlapping with lignin (approximately 1 since all of the cell wall is lignified), while M2 is the fraction of lignin overlapping with polysaccharide, a measure of the proportion of cell wall containing a particular epitope (Table II).

Colocalization of lignin and galactan epitope in compression wood yields a Pearson correlation of 0.84 (Table I) with 65% of the lignified cell wall showing significant colocalization of β(1,4)-galactan and lignin (Table II). Since LM5 binding is restricted to primary cell walls in normal wood, we did not examine colocalization with lignin in normal wood samples.

Colocalization of lignin with xylan epitopes reveals a moderate positive correlation for the LM10 epitope in normal wood, which becomes negative in compression wood (Table I). The LM11 epitope shows a weak correlation with lignin in normal wood but shows a moderate negative correlation in compression wood. The LM10 epitope overlaps with 67% of the lignified cell wall in normal wood, increasing to 76% in compression wood. The LM11 epitope overlaps with 97% of the lignified cell wall in normal wood reducing to 59% in compression wood.

The two mannan epitopes show moderate negative correlations with lignin in normal wood, but in compression wood, only LM22 continues to show this correlation (Table I). Both mannan epitopes show strong overlap with lignin in both normal and compression wood showing the greatest overall colocalization with lignin in both wood types (Table II).

In Figure 5, the differences in lignification pattern between normal and compression wood tracheids are apparent with normal wood having a highly lignified middle lamella/primary wall and a less lignified secondary wall and compression wood showing reduced lignification of the middle lamella/primary wall adjacent to intercellular spaces and increased lignification of the outer secondary wall.

The overlay images shown in Figure 5 reveal two types of colocalization between polysaccharide and lignin. For β(1,4)-galactan and lignin, there is a positive colocalization so that high galactan is associated with high lignin, which is shown as white in the overlay image (Fig. 5E) because the intensities of both signals are comparable (green + magenta = white). For all other polysaccharides, there is a negative colocalization, where high polysaccharide is associated with low lignin or vice versa, shown as magenta or green in the overlay image (Fig. 5). In the case of the LM11epitope, this negative colocalization becomes an exclusion in the S2L region of compression wood tracheids (Fig. 5G). Because all of the cell wall is lignified in tracheids, there is no occurrence of polysaccharide epitope in the absence of lignin.

Table I. *Pearson correlations for lignin/polysaccharide colocalization in normal and compression wood based on five replicate images*

Pearson correlation coefficients reflect the correlation between red and green intensities (red = epitope displayed as magenta; green = lignin, as shown in Fig. 5) for the cell wall objects in images.

Wood Type	Pearson Correlation				
	LM5	LM10	LM11	LM21	LM22
Normal wood					
1		0.31	0.22	−0.40	−0.43
2		0.39	0.09	−0.50	−0.52
3		0.31	0.22	−0.43	−0.56
4		0.31	0.11	−0.54	−0.53
5		0.45	0.06	−0.48	−0.54
Average		0.35	0.14	−0.47	−0.52
Compression wood					
1	0.81	−0.34	−0.54	0.02	−0.34
2	0.86	−0.33	−0.50	0.08	−0.30
3	0.82	−0.26	−0.54	−0.05	−0.31
4	0.86	−0.38	−0.53	−0.03	−0.34
5	0.85	−0.38	−0.50	0.05	−0.33
Average	0.84	−0.34	−0.52	0.01	−0.32

Table II. *Manders coefficients for lignin/polysaccharide colocalization in normal and compression wood*

M1 is the fraction of polysaccharide overlapping with lignin, while M2 is the fraction of lignin overlapping with polysaccharide.

Wood Type	LM5		LM10		LM11		LM21		LM22	
	M1	M2	M1	M2	M1	M2	M1	M2	M1	M2
Normal wood										
			0.98	0.63	0.99	0.99	0.98	0.75	1.00	0.66
			0.98	0.79	0.99	0.98	1.00	0.76	1.00	0.63
			0.97	0.67	0.99	0.98	0.99	0.81	1.00	0.70
			0.96	0.71	0.99	0.93	0.99	0.72	1.00	0.67
			0.98	0.54	0.99	0.96	1.00	0.73	1.00	0.74
Average			0.97	0.67	0.99	0.97	0.99	0.75	1.00	0.68
Compression wood										
	1.00	0.70	0.99	0.80	0.99	0.53	1.00	0.96	0.98	0.70
	1.00	0.70	0.99	0.77	0.98	0.62	0.99	0.98	0.97	0.97
	1.00	0.64	0.99	0.76	0.99	0.55	0.99	0.97	0.99	0.98
	1.00	0.66	0.98	0.73	0.99	0.59	1.00	0.95	0.99	0.96
	1.00	0.58	0.99	0.75	0.99	0.65	0.99	0.95	0.98	0.94
Average	1.00	0.65	0.99	0.76	0.99	0.59	0.99	0.96	0.98	0.91

Colocalization can be shown in terms of PDM (for product of the difference from the mean) images, which reveal some important details of colocalization not readily apparent from overlay images (Figs. 5 and 6). PDM images are essentially the product of the lignin image and the antibody image after segmentation at the average intensity of each image and indicate colocalization irrespective of whether such colocalization is positive or negative. In normal wood, low or unsubstituted xylans are strongly colocalized with lignin in the S1 and S3 regions of the secondary cell wall (Fig. 6A), while more highly substituted xylans are colocalized with lignin across all of the cell wall to varying extents (Fig. 6B). Mannans are colocalized with lignin in the secondary cell wall except for the S3 layer (Fig. 6, C and D).

In compression wood, galactan is strongly colocalized to the outer secondary cell wall but is excluded from other cell wall regions (Fig. 6E). Unsubstituted xylans show a weak but significant colocalization with lignin in the outer S2 region of compression wood tracheids (Fig. 6F), in contrast with the apparent exclusion of more highly substituted xylans shown by LM11 epitope in this region (Fig. 6G). By contrast, mannans show more or less equivalent colocalization in both inner and outer regions of the secondary wall of compression wood (Fig. 6, H and I) but with slightly increased colocalization at the boundary between the two regions for the LM22 epitope (Fig. 6I). This can be interpreted as high lignin × low mannan in the outer S2 region being equivalent to low lignin × high mannan in the inner S2 region. In the case of xylan, these two ratios are not equivalent, resulting in low colocalization or exclusion in the outer S2 region.

Galactan is strongly associated with increased lignification in compression wood but is almost entirely absent in normal wood. Both mannans and xylans show an inverse relationship with lignification in compression wood. By contrast, the abundance of xylan epitope is not closely related to lignification of individual wall layers in normal wood (Table I). Mannans show the most consistent relationship with lignification in both wood types, with more highly lignified wall layers having less or no mannan and less lignified layers having increased mannan.

The colocalization of polysaccharide epitopes with lignin is thus quite complex, requiring both overlay and PDM images as well as measurement of Pearson correlation and Manders overlap to fully understand the associations between these cell wall components.

Colocalization of Cellulose and Other Polysaccharides

Detection of both the LM21 and LM22 epitopes shows evidence of a radial pattern to mannan distribution in the inner S2 region of compression wood (Fig. 7A). This pattern is not obvious with xylan epitopes. Cellulose in this region of the secondary wall is known to also show such a radial organization (Donaldson, 2007), suggesting that mannan and cellulose may be more closely associated than xylan and cellulose in compression wood secondary walls. We also found evidence for an association between mannan and cellulose in delignified wood, where mannan was preferentially retained following delignification treatment, compared to galactan and xylans. It is not clear if this reflects a natural association or one induced by lignin removal.

Polarized light imaging, used to colocalize cell wall layers and crystalline cellulose with polysaccharide distribution, confirmed that xylans, especially low or unsubstituted xylans, are associated with regions of changing cellulose microfibril orientation. In normal wood tracheids, LM10 epitope is colocalized with the S1 and S3 layers, both of which have transverse cellulose microfibril orientation (Fig. 7B). In compression wood, xylans are localized to the outer margin of

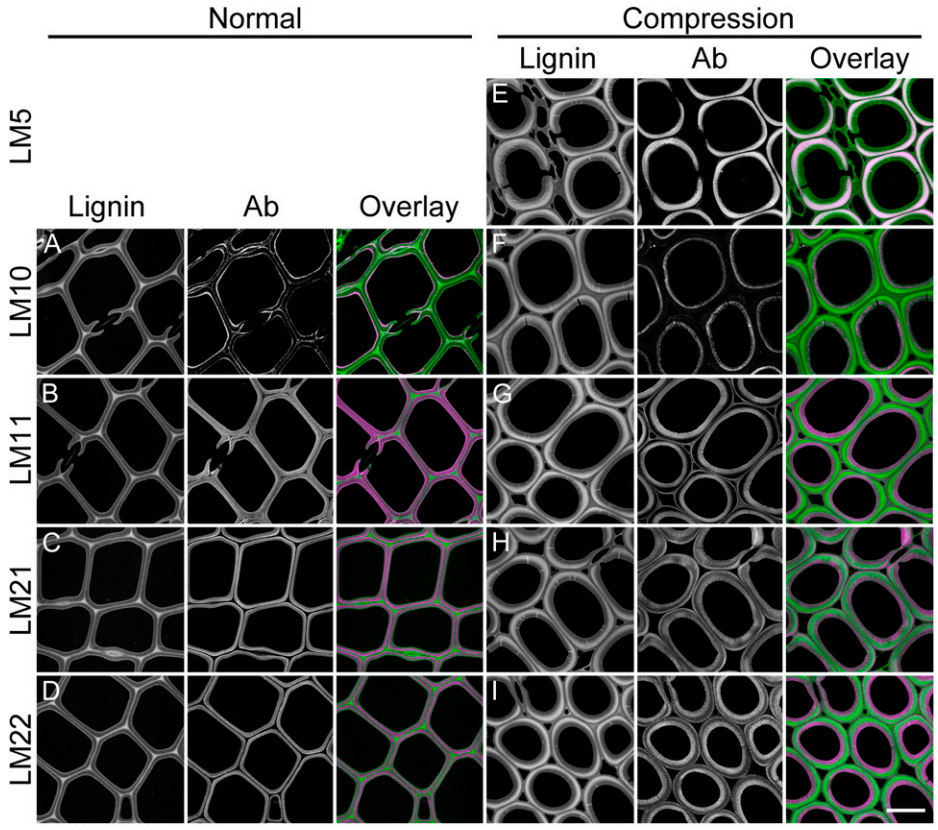

Figure 5. Detection of lignin autofluorescence and polysaccharide epitopes (Ab) in transverse sections of normal and compression wood shown as separate and overlay images. Colors in the overlay images show lignin as green and polysaccharide as magenta. Other than LM5, the distribution of most polysaccharide epitopes is an inverse image of the lignin autofluorescence intensity. A, LM10 epitope; B, LM11 epitope; C, LM21 epitope; D, LM22 epitope; E, LM5 epitope; F, LM10 epitope; G, LM11 epitope; H, LM21 epitope; I, LM22 epitope. Bar = 20 μm.

the S1 layer, where microfibrils change from the disordered primary wall to the transverse orientation of the S1 layer (Fig. 7C). Xylan is also localized to the inner S2 region where the ultrastructural organization of the wall changes relative to the outer S2 region (Fig. 7B; Donaldson, 2007). Xylans are also detected in abundance at pit borders and the dentations of ray tracheids, both areas where microfibril orientation shows complex changes (Figs. 3C and 4C).

Observations of the galactan and mannan epitopes, together with polarized light, confirmed the cell wall locations described above with no consistent relationship to microfibril orientation. Mannan epitopes localize to the S1/S2 boundary in normal wood, where microfibril orientation changes from transverse to near vertical but are absent or greatly reduced in the S3 layer, where this orientation undergoes a reversal. This would support an association of mannans with smaller microfibril angles, but in compression wood, the localization of mannan to the S1 layer conflicts with this hypothesis. Unlike xylans, mannans do not localize strongly to pit borders (Fig. 3C compared with Fig. 3I).

DISCUSSION

Galactoglucomannan is the main hemicellulose in softwood tracheids (Timell, 1967; Nanayakkara et al., 2009). The glucomannan content of compression wood is approximately 50% compared to normal wood (Nanayakkara et al., 2009). This reduced glucomannan content correlates well with the observed reduction in mannan epitopes in the outer S2 region (Fig. 3, J and L), which represents about 65% of the cell wall by area (Table II). The xylan content of compression wood is also reduced compared to that of normal wood (Timell, 1967; Nanayakkara et al., 2009), and this reduction seems to be localized to the outer S2 region with a distribution similar to mannan.

Kim et al. (2011) found that distribution of xylan epitopes in the secondary wall of compression wood in Sugi (*Cryptomeria japonica*) is more heterogeneous than for mannan epitopes. They concluded that mannan epitope distribution is uniformly reduced in compression wood relative to normal wood, in contrast with xylan epitopes, which showed a distinct reduction in the outer secondary wall of compression wood. In radiata pine, we clearly show that both mannan and xylan epitopes are reduced in the outer secondary wall of compression wood, although the reduction in xylan is more distinct. This difference in results may be due to the different antibodies used or to a lack of sensitivity of the immunogold approach relative to fluorescence, or it may reflect a difference between species. We also found some differences between mannan antibodies in the pattern of epitope detection among secondary wall layers.

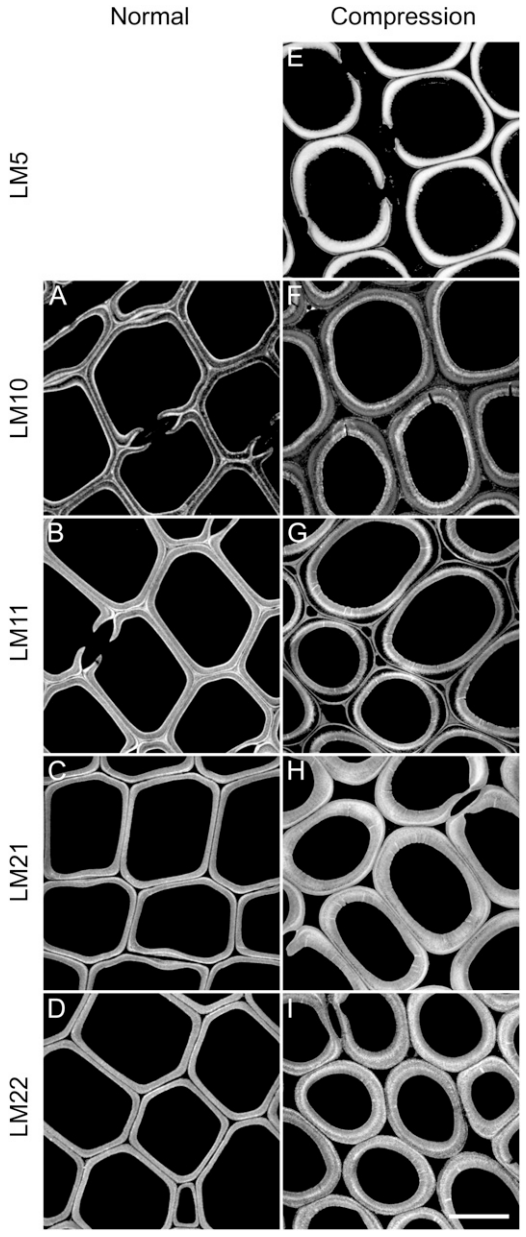

Figure 6. Colocalization of lignin and polysaccharide epitopes in transverse sections of normal and compression wood represented by PDM images. In the PDM images white indicates colocalization and black indicates exclusion. A, LM10 epitope; B, LM11 epitope; C, LM21 epitope; D, LM22 epitope; E, LM5 epitope; F, LM10 epitope; G, LM11 epitope; H, LM21 epitope; I, LM22 epitope. Bar = 20 μm.

Noncellulosic Polysaccharides Are Colocalized with Lignin in Secondary Cell Walls of Pine Xylem

Galactan has been a popular target for immunolocalization in compression wood because of its obvious relationship with increased lignification of the outer secondary wall in this wood type (Schmitt et al., 2006; Altaner et al., 2007a, 2010; Mast et al., 2009; Kim et al., 2010a). This has led to speculation that galactan may contribute to this altered lignification in some way. Interestingly, Arend (2008) has shown immunolocalization of galactan in poplar tension wood, where it seems to have a role in binding the gelatinous layer to the secondary cell wall but is not associated with lignification. In radiata pine, we observed a strong colocalization of galactan with increased lignification in the outer secondary wall region. However, we also found that the LM5 epitope is present in the S1 layer in lower amounts, where it is associated with reduced levels of lignification compared to the S2L layer (Figs. 3H and 5E). The S1 layer of compression wood is more highly lignified than in normal wood, confirming the association of galactan with increased lignification.

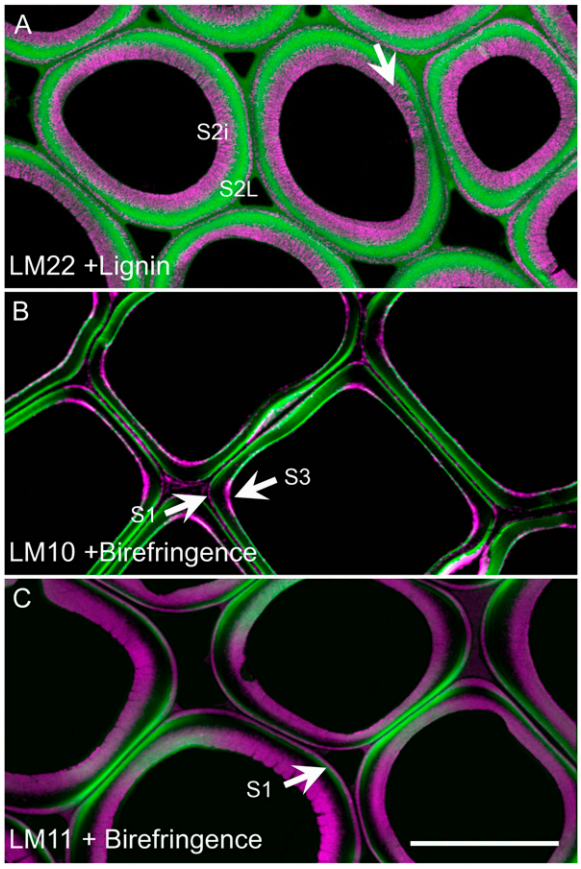

Figure 7. Overlay images of normal and compression wood in transverse section showing details of polysaccharide/lignin colocalization and xylan colocalized with birefringence. A, In compression wood tracheids, LM22 epitope (magenta) is colocalized with reduced lignification (green) in the inner S2 region (S2i) and shows a distinct radial alignment in some locations (arrow). B, In normal wood tracheids, LM10 epitope (magenta) is colocalized with birefringence (green), confirming that the epitope is abundant in the S1 and S3 layers (arrows). C, In compression wood tracheids, LM11 epitope (magenta) is localized to the outer part of the S1 layer as detected by birefringence shown in bright green (arrow) and indicating a transverse cellulose microfibril angle. LM11 epitope is also localized in the inner S2 region, which shows a stronger birefringence suggesting a more transverse orientation of cellulose microfibrils than in the outer S2 region although this is less pronounced than in the S1 layer. Bar = 20 μm.

The idea that polysaccharides, especially galactan, are in some way involved in controlling lignification has recently been extended to include mannans and xylans (Kim et al., 2010b, 2010c, 2011). These polysaccharides are known to form chemical bonds with lignin to form lignin-carbohydrate complexes (Tenkanen et al., 1999; Lawoko et al., 2005; Barakat et al., 2007), and since hemicelluloses are deposited prior to or concurrently with lignin (Kim et al., 2010a, 2010b, 2010c, 2011), the possibility that they influence lignin deposition seems reasonable. This study extends these earlier results by definitively colocalizing lignin and polysaccharides on the same field of view and measuring their association by image analysis. Our results show high correlations for galactan in compression wood and moderate correlations for mannans and xylans with some variability between normal and compression wood. Our measurements suggest a key role for mannans, which show the most consistent relationship with lignification, not only in tracheids but in other xylem cell types that undergo lignification. Ray tracheids and thick-walled ray parenchyma cells both show mannan/xylan labeling and undergo lignification, while thin-walled ray parenchyma and resin canal parenchyma do not show mannan or xylan labeling and do not undergo lignification. The observation of Altaner et al. (2007b) that the thick-walled resin canal cells of spruce (*Picea sitchensis*), which are lignified, also show labeling with both mannan and xylan antibodies, further supports this relationship. Because mannans are associated with areas of the cell wall that are less lignified (secondary walls of normal wood and the inner S2 region of compression wood), it seems possible that this polysaccharide acts by limiting the amount of lignification that takes place. Therefore, mannan is always present in lignified cell walls, but somewhat counterintuitively, it is consistently associated with reduced lignification. Unlike mannans, xylans show a relatively weak relationship with the degree of lignification, especially in normal wood. Apart from the outer secondary wall of compression wood, mannans and xylans show somewhat different distributions with each other and with lignin. By contrast, galactan is only associated with areas of increased lignification.

Based on the developmental studies of Kim et al. (2010a, 2010b, 2010c, 2011), deposition of mannan and xylan in the S1 region precedes the initial lignification of compression wood. These polysaccharides may thus act jointly as a barrier to infiltration of monolignols into the middle lamella region, resulting in the reduced lignification of the outer wall, typical of both mild and severe forms of compression wood. Reduced deposition of mannan and xylan, coupled with deposition of galactan during formation of the outer S2 region, results in increased lignification in this region. In the inner S2 region, a subsequent increase in mannan/xylan, and reduction in galactan, is associated with decreased lignification. Further studies are needed to quantify porosity changes during cell wall development to study lignin/polysaccharide/enzyme (peroxidase/laccase) localization during this process and to differentiate infiltrative and surface deposition of polysaccharides (Maeda et al., 2000; Hosoo et al., 2006; Kim et al., 2010b, 2010c).

Xylans Are Associated with Reorientation of Cellulose Microfibrils in Secondary Cell Walls of Pine Xylem

Hemicelluloses have also been proposed to have roles in controlling the orientation and clustering of cellulose microfibrils. Xylans have been associated with changes in microfibril orientation, both in polylamellate cell walls that have many alternating layers and in more conventional secondary walls, where microfibril orientation changes among the typical three layers (Reis and Vian, 2004). To extend this result to conifer tracheids, we combined immunolocalization of xylans and mannans with polarized light microscopy to show relationships with cellulose orientation. We found that xylans, especially those with low levels of substitution (LM10), show a clear association with the change from disordered to transverse orientation at the outer margin of the S1 layer (Fig. 7, B and C) and again at the S3 layer, where the near vertical orientation in the S2 region again changes to transverse relative to the fiber axis (Donaldson, 2008). A similar relationship is seen in compression wood. Xylans are also associated with pit borders (Fig. 3C) and with the dentations of ray tracheids (Fig. 4C), both regions associated with dynamic changes in microfibril orientation (Donaldson, 2008). How xylans interact with other factors involved in microfibril orientation, such as growth stress, arrangement/crowding of cellulose synthase complexes, and microtubules in the cytoskeleton (Baskin, 2001; Emons et al., 2002; Spokevicius et al., 2007; Wightman and Turner, 2008), is unknown.

It is interesting to consider experiments that could provide more direct evidence for the role of noncellulosic polysaccharides in controlling secondary wall formation. Based on our observations, down-regulation of noncellulosic polysaccharide biosynthesis using RNA interference approaches would be predicted to result in changes to both lignification and microfibril orientation, offering many opportunities for studying cell wall assembly. In Arabidopsis (*Arabidopsis thaliana*), a number of mutants have been identified that have altered xylan biosynthesis with reduced amount and altered structure expressed in xylem and interfascicular fibers (*fra8*, *irx8*, *irx9*, and *PARVUS*; Zhong et al., 2005; Persson et al., 2007; Lee et al., 2007a, 2007b). The main phenotypes observed are a reduction in fiber wall thickness and/or increased stem brittleness. Unfortunately, there is no information on wall layering and microfibril orientation in these plants. The cellulose-deficient mutant *irx3* lacks layering of the secondary wall, confirming that cellulose must be present for layers to form (Turner and Somerville, 1997).

Our results support the theories that β(1,4)-galactan is associated with increased lignification in compres-

sion wood, while mannan and to a lesser extent xylans are associated with areas of reduced lignification in both normal and compression wood, and that xylans are associated with microfibril orientation. Some discrepancies in the relative importance of mannans and xylans to the relationship with lignification as described in earlier literature may be due to differences in epitope and method (Kim et al., 2011). From other studies that demonstrate the developmental associations between polysaccharide deposition, lignifications, and secondary wall formation (Kim et al., 2010a, 2010b, 2010c, 2011), there is compelling circumstantial evidence that cell wall assembly may be mediated, at least in part, by changes in the amount and or type of polysaccharide deposited during wall formation. These theories begin to provide a simple mechanistic explanation for the structural organization of secondary cell walls.

MATERIALS AND METHODS

Sample Preparation

A radiata pine (*Pinus radiata*) tree was selected from a clonal trial planted at Rotorua, New Zealand, in 1985. The tree was bent to the ground at an early age and was swept as a result of the trees response to lean as described by Donaldson et al. (2004). Samples of mature normal (opposite wood) and compression wood were prepared for microscopy by fixation in formalin aceto-alcohol (90% ethanol, 5% glacial acetic acid, and 5% formaldehyde). The samples were stored in fixative for several months followed by washing/dehydration in ethanol and embedding in LR White acrylic resin. Samples of both wood types were also delignified in peracetic acid (35% hydrogen peroxide + glacial acetic acid, 1:1) for 4 h at 90°C, washed exhaustively in water, dehydrated in ethanol, and embedded in LR White acrylic resin. Embedded wood and holocellulose samples were sectioned in the transverse or tangential longitudinal plane at 700-nm thickness with a diamond knife, and sections were transferred to silane adhesive-coated microscope slides. Sections were dried at 70°C for 10 min and stored in the dark.

Immunofluorescence Microscopy of Cell Wall Polymers

Immunolocalization was carried out by treating sections with 0.1 mL of a 1:20 (LM5, LM10, LM11, and LM15) or 1:50 (LM21 and LM22) dilution of primary rat monoclonal antibody hybridoma cell culture supernatant in 0.1 M PBS (pH 7, containing 1% [w/v] acetylated bovine serum albumin as a blocking agent and 5 mM sodium azide) for 2 h at room temperature. Sections were then washed five times in PBS and treated with 0.1 mL of fluorescently labeled secondary antibody (goat anti-rat Alexa568; Invitrogen) in PBS at a dilution of 1:100 (20 μg/mL) for 2 h at room temperature. Sections were washed five times in PBS, rinsed in distilled water, and air dried overnight at room temperature before mounting in Citifluor immersion oil containing an antifade reagent. Control samples were prepared as above except that the primary antibody was omitted. Labeled sections and unlabeled controls were imaged at identical exposure adjusted to optimize the labeled cell walls. Sections were imaged using a Leica TCS NT confocal laser scanning microscope using 568-nm excitation and 600+ nm emission. All images are shown as maximum intensity projections.

Lignin colocalization was carried out by imaging lignin autofluorescence on the same sections labeled with LM5, LM10, LM11, LM21, or LM22. For lignin colocalization, some changes to imaging conditions were required. Because lignin autofluorescence is quenched by Alexa568, the secondary antibody label was changed to Alexa647 (goat anti-rat Alexa647; Invitrogen) with excitation at 633 nm and emission at 640 to 800 nm. To detect lignin on the same section, lignin autofluorescence was used with excitation at 457 nm and emission at 465 to 600 nm. Lignin colocalization was carried out using a Leica SP5 II spectral confocal laser scanning microscope. Controls to measure bleed-through and autofluorescence were carried out by imaging a labeled sample with excitation at 457 nm and an unlabeled sample with excitation at 633 nm using the same gain setting as a comparable labeled sample.

Enzymatic Deconstruction and Polysaccharide Masking

To study the potential effects of lignin and pectin (homogalacturonan) on detection of the LM5 and LM15 epitopes in primary cell walls of ray and resin canal tissues, a 1-year-old *P. radiata* seedling stem, 5-mm diameter, was fixed, embedded, and sectioned as described above. Sections containing phloem, cambium, and differentiating and mature xylem were sequentially treated for 2 h with 0.1 M sodium carbonate, pH 11.4, and pectinase (1 mM in sodium phosphate buffer at pH 4; Sigma-Aldrich from *Aspergillus niger*). Removal of pectic homogalacturonan was confirmed using the LM19 monoclonal antibody (Hervé et al., 2011).

Image Analysis

The colocalization between lignin and polysaccharide epitope was measured by image analysis. This involved the calculation of Pearson correlation using Digital Optics V++ software and Manders overlap coefficients (Bolte and Cordelières, 2006) using the JACoP plug-in for ImageJ software (Abramoff et al., 2004; http://rsb.info.nih.gov/ij/plugins/track/jacop.html). Overlay images combining lignin and polysaccharide signals are shown as green/magenta overlays produced with V++ software. Manually selected thresholds were used to exclude lumens from the calculation of colocalization coefficients. For comparative imaging of crystalline cellulose and cell wall layers, labeled sections were imaged for birefringence using polarization microscopy in addition to confocal fluorescence.

Determination of Binding to Pine Galactoglucommanan

Three samples of pine galactoglucomannan isolated from wood or pulp (O_2 bleached Kraft; Harwood, 1973) were hydrolyzed, and monomeric sugars were analyzed by ion chromatography (Petterson and Schwandt, 1991). Polysaccharides were examined by ELISA analysis as described by Marcus et al. (2010) to confirm binding of LM21 and LM22 to pine mannan.

ACKNOWLEDGMENTS

We thank Katrina Martin (Scion) for performing the ion chromatography analysis of pine galactoglucomannan and Susan Marcus (University of Leeds) for performing the ELISA analysis on LM21 and LM22 against pine mannan. We also thank Dr. Tim Strabala, Dr. Bernadette Nanayakkara, and Dr. David Sandquist (Scion) for critically reading and commenting on the manuscript.

Received July 26, 2011; accepted December 4, 2011; published December 5, 2011.

LITERATURE CITED

Abramoff MD, Magelhaes PJ, Ram SJ (2004) Image Processing with ImageJ. Biophotonics International **11:** 36–42

Altaner C, Hapca AI, Knox JP, Jarvis MC (2007a) Detection of β-1-4-galactan in compression wood of Sitka spruce [*Picea sitchensis* (Bong.) Carrière] by immunofluorescence. Holzforschung **61:** 311–316

Altaner C, Knox JP, Jarvis MC (2007b) In-situ detection of cell wall polysaccharides in sitka spruce (*Picea sitchensis* (Bong.) Carrière) wood tissue. BioResources **2:** 284–295

Altaner CM, Tokareva EN, Jarvis MC, Harris PJ (2010) Distribution of (1->4)-β-galactans, arabinogalactan proteins, xylans and (1->3)-β-glucans in tracheid cell walls of softwoods. Tree Physiol **30:** 782–793

Arend M (2008) Immunolocalization of (1,4)-β-galactan in tension wood fibers of poplar. Tree Physiol **28:** 1263–1267

Barakat A, Winter H, Rondeau-Mouro C, Saake B, Chabbert B, Cathala B (2007) Studies of xylan interactions and cross-linking to synthetic lignins formed by bulk and end-wise polymerization: a model study of lignin carbohydrate complex formation. Planta **226:** 267–281

Baskin TI (2001) On the alignment of cellulose microfibrils by cortical microtubules: a review and a model. Protoplasma **215:** 150–171

Bolte S, Cordelières FP (2006) A guided tour into subcellular colocalization analysis in light microscopy. J Microsc **224:** 213–232

Boraston AB, Bolam DN, Gilbert HJ, Davies GJ (2004) Carbohydrate-binding modules: fine-tuning polysaccharide recognition. Biochem J **382:** 769–781

Davin LB, Lewis NG (2005) Lignin primary structures and dirigent sites. Curr Opin Biotechnol **16:** 407–415

Donaldson LA (2001) Lignification and lignin topochemistry: an ultrastructural view. Phytochemistry **57:** 859–873

Donaldson LA (2007) Cellulose microfibril aggregates and their size variation with cell wall type. Wood Sci Technol **41:** 443–460

Donaldson LA (2008) Microfibril angle: measurement, variation and relationships. IAWA J **29:** 345–386

Donaldson LA (2009) Immunocytochemistry of wood cell walls: a review. N Z J For Sci **39:** 161–168

Donaldson LA, Grace JC, Downes G (2004) Within tree variation in anatomical properties of compression wood in radiata pine. IAWA J **25:** 253–271

Emons A-MC, Schel JHN, Mulder BM (2002) The geometric model for microfibril deposition and the influence of the cell wall matrix. Plant Biol **4:** 22–26

Fernando D, Daniel G (2008) Exploring Scots pine fibre development mechanisms during TMP processing: impact of cell wall ultrastructure (morphological and topochemical) on negative behaviour. Holzforschung **62:** 597–607

Filonova L, Gunnarsson LC, Daniel G, Ohlin M (2007) Synthetic xylan-binding modules for mapping of pulp fibres and wood sections. BMC Plant Biol **7:** 54

Hannuksela T, Tenkanen M, Holmborn B (2002) Sorption of dissolved galactoglucomannans to bleached kraft pulp. Cellulose **9:** 251–261

Harwood VD (1973) Studies on the cell wall polysaccharides of *Pinus radiata*. 11. Structure of a glucomannan. Svensk Papperstidning **76:** 377–379

Hervé C, Marcus SE, Knox JP (2011) Monoclonal antibodies, carbohydrate-binding modules, and the detection of polysaccharides in plant cell walls. Methods Mol Biol **715:** 103–113

Hosoo Y, Imai T, Yoshida M (2006) Diurnal differences in the supply of glucomannans and xylans to innermost surface of cell walls at various developmental stages from cambium to mature xylem in *Cryptomeria japonica*. Protoplasma **229:** 11–19

Hsieh YSY, Paxton M, Ade CP, Harris PJ (2009) Structural diversity, functions and biosynthesis of xyloglucans in angiosperm cell walls. N Z J For Sci **39:** 187–196

Iwata T, Indrarti L, Azuma J-I (1998) Affinity of hemicellulose for cellulose produced by *Acetobacter xylinum*. Cellulose **5:** 215–228

Jones L, Seymour GB, Knox JP (1997) Localization of pectic galactan in tomato cell walls using a monoclonal antibody specific to (1→4)-β-D-galactan. Plant Physiol **113:** 1405–1412

Kim JS, Awano T, Yoshinaga A, Takabe K (2010a) Immunolocalization of β-1-4-galactan and its relationship with lignin distribution in developing compression wood of *Cryptomeria japonica*. Planta **232:** 109–119

Kim JS, Awano T, Yoshinaga A, Takabe K (2010b) Temporal and spatial immunolocalization of glucomannans in differentiating earlywood tracheid cell walls of *Cryptomeria japonica*. Planta **232:** 545–554

Kim JS, Awano T, Yoshinaga A, Takabe K (2010c) Immunolocalization and structural variations of xylan in differentiating earlywood tracheid cell walls of *Cryptomeria japonica*. Planta **232:** 817–824

Kim JS, Awano T, Yoshinaga A, Takabe K (2011) Occurrence of xylan and mannan polysaccharides and their spatial relationship with other cell wall components in differentiating compression wood tracheids of *Cryptomeria japonica*. Planta **233:** 721–735

Kimura S, Laosinchai W, Itoh T, Cui X, Linder CR, Brown RM Jr (1999) Immunogold labeling of rosette terminal cellulose-synthesizing complexes in the vascular plant vigna angularis. Plant Cell **11:** 2075–2086

Knox JP (2008) Revealing the structural and functional diversity of plant cell walls. Curr Opin Plant Biol **11:** 308–313

Lairez D, Cathala B, Monties B, Bedos-Belval F, Duran H, Gorrichon L (2005) Aggregation during coniferyl alcohol polymerization in pectin solution: a biomimetic approach of the first steps of lignification. Biomacromolecules **6:** 763–774

Lawoko M, Henriksson G, Gellerstedt G (2005) Structural differences between the lignin-carbohydrate complexes present in wood and in chemical pulps. Biomacromolecules **6:** 3467–3473

Lee C, O'Neill MA, Tsumuraya Y, Darvill AG, Ye Z-H (2007a) The irregular xylem9 mutant is deficient in xylan xylosyltransferase activity. Plant Cell Physiol **48:** 1624–1634

Lee C, Zhong R, Richardson EA, Himmelsbach DS, McPhail BT, Ye Z-H (2007b) The *PARVUS* gene is expressed in cells undergoing secondary wall thickening and is essential for glucuronoxylan biosynthesis. Plant Cell Physiol **48:** 1659–1672

Maeda Y, Awano T, Takabe K, Fujita M (2000) Immunolocalisation of glucomannans in the cell wall of differentiating tracheids in *Chamaecyparis obtusa*. Protoplasma **213:** 148–156

Marcus SE, Blake AW, Benians TAS, Lee KJD, Poyser C, Donaldson L, Leroux O, Rogowski A, Petersen HL, Boraston A, et al (2010) Restricted access of proteins to mannan polysaccharides in intact plant cell walls. Plant J **64:** 191–203

Marcus SE, Verhertbruggen Y, Hervé C, Ordaz-Ortiz JJ, Farkas V, Pedersen HL, Willats WGT, Knox JP (2008) Pectic homogalacturonan masks abundant sets of xyloglucan epitopes in plant cell walls. BMC Plant Biol **8:** 60

Mast SW, Donaldson LA, Torr K, Phillips L, Flint H, West M, Strabala TJ, Wagner A (2009) Exploring the ultrastructural localization and biosynthesis of β(1,4)-galactan in *Pinus radiata* compression wood. Plant Physiol **150:** 573–583

McCartney L, Marcus SE, Knox JP (2005) Monoclonal antibodies to plant cell wall xylans and arabinoxylans. J Histochem Cytochem **53:** 543–546

Melton LD, Smith BG, Ibrahim R, Schröder R (2009) Mannans in primary and secondary plant cell walls. N Z J For Sci **39:** 153–160

Mishima T, Hisamatsu M, York WS, Teranishi K, Yamada T (1998) Adhesion of β-D-glucans to cellulose. Carbohydr Polym **308:** 389–395

Nanayakkara B, Manley-Harris M, Suckling ID, Donaldson LA (2009) Quantitative chemical indicators to assess the gradation of compression wood. Holzforschung **63:** 431–439

Persson S, Caffall KH, Freshour G, Hilley MT, Bauer S, Poindexter P, Hahn MG, Mohnen D, Somerville C (2007) The *Arabidopsis* irregular xylem8 mutant is deficient in glucuronoxylan and homogalacturonan, which are essential for secondary cell wall integrity. Plant Cell **19:** 237–255

Petterson RC, Schwandt VH (1991) Wood sugar analysis by anion chromatography. J Wood Chem Technol **11:** 495–501

Putoczki TL, Gerrard JA, Butterfield BG, Jackson SL (2008) The distribution of un-esterified and methyl-esterified pectic polysaccharides in *Pinus radiata*. IAWA J **29:** 115–127

Putoczki TL, Pettolino F, Griffin MDW, Möller R, Gerrard JA, Bacic A, Jackson SL (2007) Characterization of the structure, expression and function of *Pinus radiata* D. Don arabinogalactan-proteins. Planta **226:** 1131–1142

Ralph J, Brunow G, Harris PJ, Dixon RA, Schatz PF, Boerjan W (2008) Lignification: Are lignins biosynthesized via simple combinatorial chemistry or via proteinaceous control and template replication? *In* F Daayf, A El Hadrami, L Adam, GM Balance, eds, Recent Advances in Polyphenol Research, Vol 1. Wiley-Blackwell Publishing, Oxford, UK, pp 36–66

Reis D, Vian B (2004) Helicoidal pattern in secondary cell walls and possible role of xylans in their construction. C R Biol **327:** 785–790

Schmitt U, Singh A, Frankenstein C, Möller R (2006) Cell wall modifications in woody stems induced by mechanical stress. N Z J For Sci **36:** 72–86

Spokevicius AV, Southerton SG, MacMillan CP, Qiu D, Gan S, Tibbits JFG, Moran GF, Bossinger G (2007) β-tubulin affects cellulose microfibril orientation in plant secondary fibre cell walls. Plant J **51:** 717–726

Tanahashi M, Higuchi T (1990) Effect of the hydrophobic regions of hemicelluloses on dehydrogenative polymerisation of synapyl alcohol. Mokuzai Gakkaishi **36:** 424–428

Tenkanen M, Tamminen T, Hortling B (1999) Investigation of lignin-carbohydrate complexes in kraft pulps by selective enzymatic treatments. Appl Microbiol Biotechnol **51:** 241–248

Timell TE (1967) Recent progress in the chemistry of wood hemicelluloses. Wood Sci Technol **1:** 45–70

Timell TE (1986) Chemical properties of compression wood. *In* Compression Wood in Gymnosperms, Vol 1. Springer-Verlag, Berlin, pp 289–408

Turner SR, Somerville CR (1997) Collapsed xylem phenotype of *Arabidopsis* identifies mutants deficient in cellulose deposition in the secondary cell wall. Plant Cell **9:** 689–701

Wardrop AB, Preston RD (1947) Organization of the cell walls of tracheids and wood fibres. Nature **160:** 911–913

Wightman R, Turner SR (2008) The roles of the cytoskeleton during cellulose deposition at the secondary cell wall. Plant J **54:** 794–805

Willats WGT, Steele-King CG, McCartney L, Orfila C, Marcus SE, Knox JP (2000) Making and using antibody probes to study plant cell walls. Plant Physiol Biochem **38:** 27–36

Yoshida S, Tanahashi M, Shigematsu M, Shinoda Y (1994) Effect of reaction medium on dehydrogenative polymerization of sinapyl alcohol. Mokuzai Gakkaishi **40:** 974–979

Zhong R, Peña MJ, Zhou G-K, Nairn CJ, Wood-Jones A, Richardson EA, Morrison WH III, Darvill AG, York WS, Ye Z-H (2005) *Arabidopsis* fragile fiber8, which encodes a putative glucuronyltransferase, is essential for normal secondary wall synthesis. Plant Cell **17:** 3390–3408